

Article

Analysis of Photo-Generated Carrier Escape in Multiple Quantum Wells

Jiaping Guo¹, Weiye Liu¹, Ding Ding¹, Xinhui Tan¹, Wei Zhang¹ , Lili Han¹, Zhaowei Wang¹, Weihua Gong¹, Jiyun Li¹, Ruizhan Zhai¹, Zhongqing Jia¹, Ziguang Ma², Chunhua Du³, Haiqiang Jia³ and Xiansheng Tang^{1,*}

¹ Laser Institute, Qilu University of Technology (Shandong Academy of Sciences), Jinan 250014, China

² Huawei Technologies Co., Ltd., Beijing 100095, China

³ Institute of Physics, Chinese Academy of Sciences, Beijing 100083, China

* Correspondence: 18811681359@163.com; Tel.: +86-188-1168-1359

Abstract: Recent experiments have shown that more than 85% of photo-generated carriers can escape from multiple quantum wells (MQWs) sandwiched between p-type and n-type layers (PIN). In this work, we quantitatively analyze the relationship between the energy of carriers and the height of potential barriers to be crossed, based on the GaAs/InGaAs quantum well structure system, combined with the Heisenberg uncertainty principle. It was found that the energy obtained by electrons from photons is just enough for them to escape, and it was found that the energy obtained by the hole is just enough for it to escape due to the extra energy calculated, based on the uncertainty principle. This extra energy is considered to come from photo-generated thermal energy. The differential reflection spectrum of the structure is then measured by pump-probe technology to verify the assumption. The experiment shows that the photo-generated carrier has a longer lifetime in its short circuit (SC) state, and thus it possesses a lower structure temperature than that in open circuit (OC). This can only explain a thermal energy reduction caused by the continuous carrier escape in SC state, indicating an extra thermal energy transferred to the escaping carriers. This study is of great significance to the design of new optoelectronic devices and can improve the theory of photo-generated carrier transports.

Keywords: photo-generated carriers; escape; uncertainty principle



Citation: Guo, J.; Liu, W.; Ding, D.; Tan, X.; Zhang, W.; Han, L.; Wang, Z.; Gong, W.; Li, J.; Zhai, R.; et al.

Analysis of Photo-Generated Carrier Escape in Multiple Quantum Wells. *Crystals* **2023**, *13*, 834. <https://doi.org/10.3390/cryst13050834>

Academic Editor: Paolo Olivero

Received: 14 April 2023

Revised: 14 May 2023

Accepted: 16 May 2023

Published: 17 May 2023



Copyright: © 2023 by the authors. Licensee MDPI, Basel, Switzerland. This article is an open access article distributed under the terms and conditions of the Creative Commons Attribution (CC BY) license (<https://creativecommons.org/licenses/by/4.0/>).

1. Introduction

Semiconductor materials are the cornerstones of the information society, and the progress of science and technology cannot be separated from the development of semiconductor materials and processes. In addition to the important applications in the field of electronics, semiconductor materials also have high application potential in the field of optoelectronics. With the advancement of semiconductor theory and manufacturing technology, quantum well (QW) and super-lattice structures have been developed. The quantum well structure has played an important role in the field of electricity-to-light conversion since its invention [1–9]. Light-emitting diodes (LEDs) [10–12] and lasers [13–15] both adopt multi-quantum well (MQW) structures due to their strong carrier capture and confinement capabilities in the electricity-to-light conversion field. These two devices achieved good commercial applications, and they are gradually changing and enriching people's lives. As a new generation of lighting sources, LEDs have been gradually replacing incandescent light sources. The laser is more widely used in industrial, military, and other fields. However, as for the light-to-electricity conversion, the use of low-dimensional structures is somewhat limited. Quantum well infrared detectors (QWIPs) are the most widely used structures [16–18], which mainly exploit transitions between sub-bands. However, MQWs are hard to apply in light-to-electricity conversion devices based on the inter-band transition because, according to the classical theory, the photo-generated carriers would relax to the ground state of the low-dimensional materials, from where the photo-generated

carriers cannot escape to form a photocurrent due to quantum confinement [19]. Due to quantum confinement, the carriers in quantum wells can only disappear through relaxation and recombination and cannot escape. Therefore, the application of low-dimensional semiconductor structure in the field of photoelectric conversion is limited.

Recently, many research groups have found that most part of photo-generated carriers would escape from MQWs when the MQWs' structures are placed in the depletion region of the PN junction (PIN structure) [20–23]. By measuring the photoluminescence (PL) spectra in the case of open circuits (OCs) and short circuits (SCs), respectively, it was found that there is an obvious fluorescence quenching in the case of SC, accompanied by obvious photocurrent production [24–28]. This new phenomenon breaks our understanding of the carrier limiting effect of traditional low-dimensional structures. This shows that the photo-generated carriers can escape efficiently and can be used in photo-electric conversion devices. Furthermore, this phenomenon is not special and can be found in many material systems. We have investigated a large number of low dimensional material systems, including GaN/InGaN quantum well structures [21], GaAs/InGaAs quantum well structures [20], and GaAs/InAs quantum dot (QD) structures [29], all of which indicate that, when the thickness of the MQWs structure region is less than 100 nm, more than 85% of carriers can escape by comparing their integral strength of the PL peak under the OC and SC states. This special structure can be used to make new types of optoelectronic devices, such as quantum well solar cells and photodetectors (IQWIP) [25,30], which widen the range of applications of quantum wells. Meanwhile, as for the NIN structure that the MQW structures are placed into in the depletion region of the NN junction (NIN structure), there is no obvious fluorescence quenching phenomenon in the case of SC, even if bias voltage is applied [21,22,31]. Furthermore, this large escape rate cannot be explained by tunneling theory or thermionic emission theory. These theories can only explain some special structures in the special cases, but they cannot cover all cases. In some cases, a combination of the two theories is needed to explain a particular situation. Therefore, these two theories are not complete and need new interpretation. In this paper, we quantitatively analyze the relationship between the energy of carriers and the height of potential barriers to be crossed, based on the GaAs/InGaAs MQWs structure system of ref. [20], combined with the Heisenberg uncertainty principle [32]. We compared the energy difference between the energy level and the energy obtained by the excited carriers. The energy is analyzed from a quantitative point of view, and, combined with the energy introduced by the uncertainty principle, further numerical comparison is made. Based on the above analysis, some energy sources are guessed, and the pump–probe technique was applied to verify our relevant hypotheses. This study is of great significance to the design of new optoelectronic devices and can improve the theory of photo-generated carrier transport.

2. Analysis and Discussion

The PIN structure investigated in this work is based on GaAs/InGaAs MQWs structure [20]. Its epitaxial structure and energy band structure are shown in Figure 1a. The structure includes 10 quantum wells of InGaAs with thickness of 5 nm, and the composition of indium is 0.2. The width of barrier of GaAs is 20 nm. Figure 1 shows the energy band diagrams of PIN structure, the corresponding MQWs structure, and the sub-band energies, respectively. It can be seen that the conduction band level of GaAs is 0.6242 eV, and the valence band level is -0.7951 eV, showing that the band gap is 1.42 eV, which is consistent with the classical data of GaAs at 300 K. From Figure 1b, we can see that the conduction band level of In(0.2)GaAs is 0.4765 eV, and the valence band level is -0.7115 eV; for the electron, the first confined energy level in the well is 0.5424 eV, and, for the hole, the first confined energy level in the well is -0.7264 eV. This shows a band gap of 1.27 eV between two confined energies, corresponding to an emission wavelength of 976 nm, which is almost in agreement with that reported in [20]. Here, the strain is not considered in the calculation process, and the thickness of samples grown in the experiment is associated

with a fluctuation, which results in a 6 nm wavelength fluctuation. So, this calculation is acceptable.

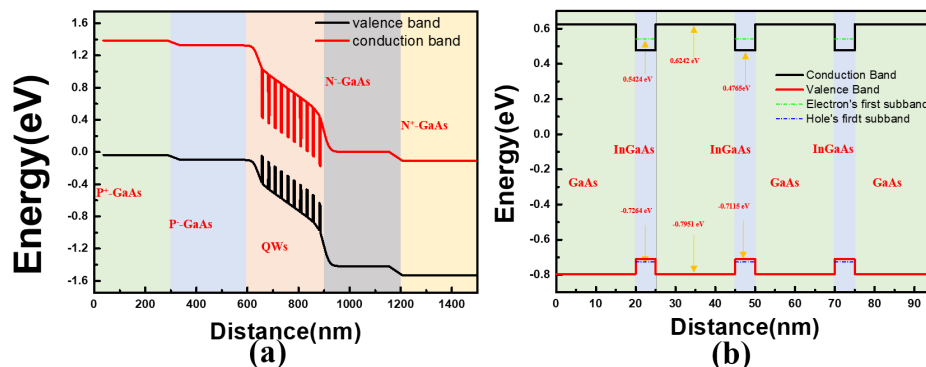


Figure 1. (a) Band diagram of the PIN structure. (b) Band diagram of ordinary quantum well structures.

According to the above data, we can find that the energy difference between the electron’s first confined energy level and the energy of the barrier level of the electron is 81.8 meV, and the energy difference between the hole’s first confined energy level and the energy of the barrier level of the hole is 68.7 meV. The energy difference between the energy of barrier level of the electron and the hole’s first confined energy level is 1.35 eV, which corresponds to an excitation wavelength of 918 nm. When an excitation wavelength of 915 nm is used [20], the photon energy is greater than 1.355 eV. Therefore, the excited electrons with enough energy can escape directly. Additionally, electrons are not localized in quantum wells. So, we only need to consider the energy of excited holes.

The hole could also gain energy through the scattering from carriers and lattice, though the whole energy of the incident photon is carried away by the electron through the transition. The average thermal equilibrium energy of a large number of particles can be obtained by equilibrium theory. Additionally, the energy per free dimension is $1/2 kT$, where k represents the Boltzmann constant, and T represents the absolute temperature. The carrier only has two free dimensions in the confined energy level. So, the energy of the hole obtained from carriers or lattices by scattering is kT . However, the above relevant experiments have shown that confined carriers can escape from MQWs in the PIN structure, which showed the properties of free carriers in three dimensions. Therefore, the hole would have three free dimensions, and the resulting energy is $3/2 kT$, which is 39 meV at room temperature.

It should be noted that there is a strong built-in electric field in the depletion region of the PN junction, which will accelerate the hole to obtain a certain velocity. The simulated distribution of the electric field in the structure is shown in Figure 2a. It can be seen that the electric field intensity in the MQW region is greater than 2×10^4 V/cm. From Figure 2b, we can see the relationship between the carrier saturation drift velocity and the electric field intensity in the GaAs material system is based on equations. The saturation drift velocity of holes increases with the increase in electric field intensity, eventually approaching to 10^7 cm/s. There exists velocity overshoot due to very short acceleration time of the hole in the MQWs. Meanwhile, due to the separation energy level in the quantum wells, the scattering effect of the hole will be reduced, so its saturation velocity will also increase. We treated the saturation velocity of the cavity in the well as 10^7 cm/s. Therefore, the kinetic energy obtained by the hole from the electric field is $1/2 mv^2$, corresponding to 17 meV. Combined with the above 39 meV thermal energy, the current total energy obtained is 56 meV, which is still less than the 68.7 meV that needs to be crossed. So, we need to think about other forms of energy.

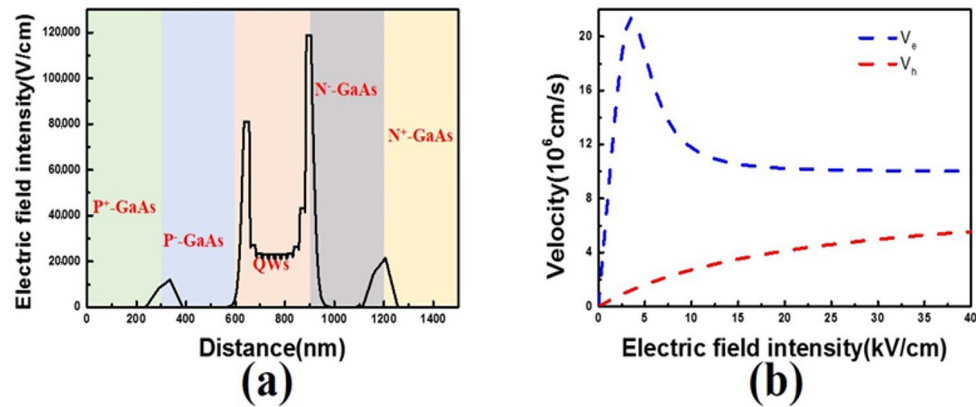


Figure 2. (a) Electric field intensity distribution in the PIN structure. (b) Variation of carrier saturation drift velocity vs. electric field intensity in GaAs.

Since holes also have quantum properties, we consider the energy due to uncertainty relations. Finally, according to the Heisenberg uncertainty principle $\Delta E \Delta t \geq \hbar/2$, where ΔE represents the difference between the measured energy and the actual energy, and Δt , the difference between the measured time and the actual time, \hbar reduced Planck's constant. The width of the well is known to be 5 nm, and the velocity of the hole is 10^7 cm/s, giving an average escape time of the hole of 25 fs. It has been confirmed, from previous experiments, that the escape time of photo-generated carriers is on the order of femtoseconds to picoseconds. This is in good agreement with the reported data [31], and it is accurate in terms of magnitude. Now that the time is accurate, the energy uncertainty ΔE can be estimated by substituting the time and the reduced Planck's constant, which is ~ 13 meV.

From the above analysis, we can see that the energy of the hole contains thermal energy (39 meV), kinetic energy (17 meV), and uncertain energy (13 meV). Therefore, the hole in the quantum wells in the PIN structure has an energy of 69 meV, which is just larger than the barrier potential of 68.7 meV. This implies that, after considering the energy introduced by the uncertainty principle, the hole can escape from the MQWs. So, both holes and electrons can escape from the PIN structure and enter the external circuit, which results in fluorescence quenching in the case of SC. Additionally, here, we have a quantitative explanation of why photo-generated carriers can escape to MQWs.

For the state of OC, both sides of the wafer accumulate different carriers, which would introduce a new electric field, whose direction is different than that of the built-in electric field of the PN junction, as shown in Figure 3a, making the hole lose part of the energy source.

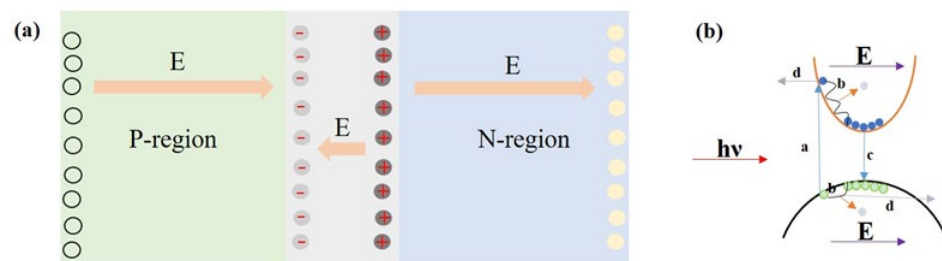


Figure 3. (a) The electric field inside the structure under OC. (b) Four processes that photo-generated carriers go through.

Since the electric field formed by the accumulation of charge carriers on both sides of the epitaxial structure is not damaged by the outside cases, and the surface-composite charge carriers are constantly supplemented by the internal photo-generated carriers, this

maintains the stability of the electric field. The holes cannot obtain enough energy for continuous escape, which makes the fluorescence intensity still strong in the OC state, even in the case of escape. From Figure 3b, we can see that there are four processes for photo-generated carriers in the PIN structure: generation, relaxation, recombination, and escape. Although the time for photo-generated carriers to escape from a quantum well is on the order of femtoseconds, it is on the order of picoseconds for the MQW region, with a width of hundreds of nanometers or even microns. The photo-generated carriers either escape or undergo radiative recombination. It has been proven that the carrier escapes first [28]. The fluorescence intensity is consistent with that of OC when a bias voltage equivalent to the built-in electric field is applied. This fully indicates that the existence of escaping carriers reduces the built-in electric field. So, photogenic carriers cannot escape continuously.

According to the conservation of energy, the uncertain energy obtained by the hole should also be converted from another energy source. It is preliminarily speculated that this part of the energy comes from photon energy that fails to generate carriers by excitation, that is, heat energy. Next, we designed an experiment to verify this hypothesis.

It is well known that the lifetime of carriers decreases with temperature increase. Therefore, we can compare the lifetime of the carriers to explore the local surface temperature of the sample. Photo-generated carriers are a kind of non-equilibrium carrier. Their behavior follows a certain statistical theory. In general, the decay is exponential. The concentration of photo-generated carriers will affect the reflectance of the sample surface. Therefore, the carrier lifetime can be detected by measuring the differential reflection spectrum, based on the pump–probe technique. The pump–probe technique was first proposed by Toepfer. Two femtosecond (fs) pulses, with time delay, are used, in which the one with higher energy and earlier time is used as the pump light, while the one with lower energy and later time is used as the probe light to excite and probe the samples, respectively. The pump light and the probe light are obtained by the same femtosecond laser beam passing through the beam splitter mirror, with one beam of high energy as the pump light and the other beam of low energy as the probe light. After the probe light passes through a displacement platform, there will be an optical path difference between the probe light and the pump light, and then a certain time interval will be generated. This is performed so that they can reach the surface of the sample successively. The pump light excites the sample to the excited state, and the probe light with time delay arrives later. The probe sample evolves with time after being excited. Figure 4a shows the schematic diagram of the pump–probe technology. The laser used has a wavelength of 808 nm with 1 kHz repetition frequency and 1 mW energy. The pulsed laser beam passed through a polarization beam splitter (PBS), which was divided into two pulsed beams, pump and probe, with an energy ratio of 10:1. The pump light shines on the sample, which is consistent with ref. [20], after passing through a corner reflector, which is mounted on a step motor. Therefore, the optical path difference between the pump light and the probe light, i.e., the time difference between the two pulsed light beams arriving at the sample surface, can be adjusted. The surface reflectivity of the sample is measured by using probe light with and without pump excitation, respectively, so that the differential reflection spectrum is obtained. The photon energy, corresponding to 808 nm wavelength, is larger than the band gap of GaAs and the band gap of InGaAs in the quantum well, so the photo-generated carriers can be excited simultaneously in the quantum well and on the surface. By studying the dynamic behavior of surface photo-generated carriers, the lifetime and local temperature variation are determined. The same measurement was carried out while the sample was further heated with a 532 nm laser for the purpose of enhancing the measurement contrast. By setting the sample to OC state and SC state with and without laser heating, we obtain the measurement results, which are shown in Figure 4b, which shows the lifetime of photo-generated carriers under different condition.

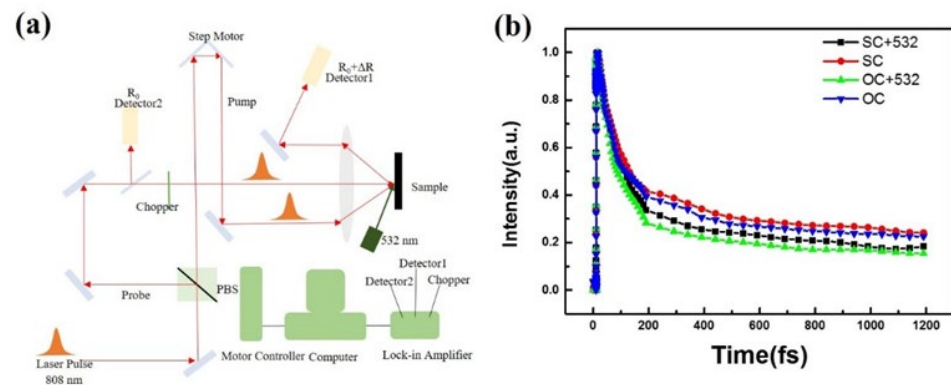


Figure 4. (a) Physical diagram of the optical path of pump-probe technology. (b) Differential reflection spectra of samples in different states.

From Figure 4b, it can be seen that the lifetime of the SC state is longer than that of the OC state, showing that the sample temperature of SC state is lower than that of the OC state. It has been reported that, under the condition of SC, most photo-excited carriers escape from the quantum wells to generate photo-excited current, rather than relax to the ground state of quantum wells and recombine to emit light [20]. Since holes need energy to escape in the SC state, the heat energy may provide this excess energy, giving rise to a lower sample temperature than that in OC state. In the OC state, the sample temperature is higher due to no continuous escape phenomena.

When 532 nm laser heating is applied, both lifetimes of photo-generated carriers under OC and SC conditions become smaller, but they show the same trend, indicating a higher sample temperature induced by light heating. In this case, however, the lifetime of the SC state still is longer than that of the OC state. From the lifetime of the carrier in different states, one can deduce that the heat generated by light makes a contribution to the carrier escape in the SC state, resulting in a lower sample temperature than that in the OC state. This implies that heat generated by light may provide excess energy for carrier escape in the SC state.

3. Conclusions

In this paper, we mainly analyzed the energy of the hole from multiple aspects. In terms of this specific structure and the photo excitation source used (915 nm), we can know that the photo-generated electron can escape from quantum wells with enough energy. The energy uncertainty of the hole is calculated (13 meV), based on the uncertainty principle. Combined with thermal energy (39 meV) and kinetic energy (17 meV), we can find that the energy of the hole is 69 meV, which is greater than the barrier potential of 68.7 meV. This implies that the hole has enough energy to escape. We have assumed that the excess energy comes from the photon that has not excited the carriers, that is, photo-generated heat energy, and we verified this by using pump-probe technology. It has been found that, in the SC state, energy is required for carriers to escape, and this excess energy comes from light heating energy, so the sample temperature in this state is lower than that of the OC state, and the lifetime of carriers is longer than that of the OC state. In the OC state, the sample temperature is higher because of the lack of continuous escape phenomenon, and the lifetime of carriers is shorter. The conclusion of this work would help better understand the design of new solar cells, photodetectors, and other photoelectric devices, which are based on MQWs. It also provides a complement to the transport theory of photo-generated carriers.

Author Contributions: Conceptualization, R.Z., Z.J., Z.M., C.D., H.J. and X.T. (Xiansheng Tang); methodology, Z.M., C.D., H.J. and X.T. (Xiansheng Tang); software, X.T. (Xiansheng Tang); validation, W.Z., L.H., Z.W., W.G. and J.L.; formal analysis, X.T. (Xiansheng Tang); investigation, X.T. (Xiansheng Tang); resources, X.T. (Xiansheng Tang), W.Z., L.H. and Z.W.; data curation, X.T. (Xiansheng Tang); writing—original draft preparation, J.G., W.L., D.D. and X.T. (Xinhui Tan); writing—review and editing, X.T. (Xiansheng Tang). All authors have read and agreed to the published version of the manuscript.

Funding: This work was supported by National Key research and development Program (Grant No. 2021YFB3201904). This work was supported by National Natural Science Foundation of China (No. 62005138). This work was supported by Qilu University of Technology (Shandong Academy of Sciences) Peixin fund project (Grant No. 2022PX080). This work was supported by Qilu University of Technology (Shandong Academy of Sciences) International Cooperation Projects (Grant No. 2022GH001). This work was also supported by Qilu University of Technology (Shandong Academy of Sciences) Computer Science and Technology “Four Plans” talent introduction and Multiplication plan project (Grant No. 2021YY01002) and supported by the Youth fund of the Shandong Natural Science Foundation (Grant Nos. ZR2020QF098 and ZR2022QF115). This work was also supported by Project of Jinan (Grant No. 2020GXRC032).

Data Availability Statement: Data are available upon request from the authors.

Conflicts of Interest: The authors declare no conflict of interest.

References

1. Bushnell, D.B.; Tibbits, T.N.D.; Barnham, K.W.J.; Connolly, J.P.; Mazzer, M.; Ekins-Daukes, N.J.; Roberts, J.S.; Hill, G.; Airey, R. Effect of well number on the performance of quantum-well solar cells. *J. Appl. Phys.* **2005**, *97*, 124908. [[CrossRef](#)]
2. Courel, M.; Rimada, J.C.; Hernández, L. GaAs/GaN quantum well and superlattice solar cell. *Appl. Phys. Lett.* **2012**, *100*, 073508. [[CrossRef](#)]
3. Wang, S.; Long, H.; Zhang, Y.; Chen, Q.; Dai, J.; Zhang, S.; Chen, J.; Liang, R.; Xu, L.; Wu, F.; et al. Monolithic integration of deep ultraviolet LED with a multiplicative photoelectric converter. *Nano Energy* **2019**, *66*, 104181. [[CrossRef](#)]
4. Elahi, E.; Suleman, M.; Nisar, S.; Sharma, P.R.; Iqbal, M.W.; Patil, S.A.; Kim, H.; Abbas, S.; Chavan, V.D.; Dastgeer, G.; et al. Robust approach towards wearable power efficient transistors with low subthreshold swing. *Mater. Today Phys.* **2022**, *30*, 100943. [[CrossRef](#)]
5. Dastgeer, G.; Nisar, S.; Shahzad, Z.M.; Rasheed, A.; Kim, D.K.; Jaffery, S.H.A.; Eom, J. Low-Power Negative-Differential-Resistance Device for Sensing the Selective Protein via Supporter Molecule Engineering. *Adv. Sci.* **2023**, *10*, 2204779. [[CrossRef](#)] [[PubMed](#)]
6. Dastgeer, G.; Shahzad, Z.M.; Chae, H.; Kim, Y.H.; Ko, B.M.; Eom, J. Bipolar Junction Transistor Exhibiting Excellent Output Characteristics with a Prompt Response against the Selective Protein. *Adv. Funct. Mater.* **2022**, *32*, 2204781. [[CrossRef](#)]
7. Dastgeer, G.; Afzal, A.M.; Aziz, J.; Hussain, S.; Jaffery SH, A.; Kim, D.K.; Assiri, M.A. Flexible memory device composed of metal-oxide and two-dimensional material (SnO₂/WTe₂) exhibiting stable resistive switching. *Materials* **2021**, *14*, 7535. [[CrossRef](#)] [[PubMed](#)]
8. Dastgeer, G.; Afzal, A.M.; Jaffery, S.H.A.; Imran, M.; Assiri, M.A.; Nisar, S. Gate modulation of the spin current in graphene/WSe₂ van der Waals heterostructure at room temperature. *J. Alloys Compd.* **2022**, *919*, 165815. [[CrossRef](#)]
9. Dastgeer, G.; Afzal, A.M.; Nazir, G.; Sarwar, N. p-GeSe/n-ReS₂ heterojunction rectifier exhibiting a fast photoresponse with ultra-high frequency-switching applications. *Adv. Mater. Interfaces* **2021**, *8*, 2100705. [[CrossRef](#)]
10. Yeh, D.-M.; Huang, C.-F.; Chen, C.-Y.; Lu, Y.-C.; Yang, C.C. Surface plasmon coupling effect in an InGaN/GaN single-quantum-well light-emitting diode. *Appl. Phys. Lett.* **2007**, *91*, 171103. [[CrossRef](#)]
11. Yadav, G.; Dewan, S.; Tomar, M. Electroluminescence study of InGaN/GaN QW based p-i-n and inverted p-i-n junction based short-wavelength LED device using laser MBE technique. *Opt. Mater.* **2022**, *126*, 112149. [[CrossRef](#)]
12. Ahmad, S.; Raushan, M.; Kumar, S.; Dalela, S.; Siddiqui, M.; Alvi, P. Modeling and simulation of GaN based QW LED for UV emission. *Optik* **2018**, *158*, 1334–1341. [[CrossRef](#)]
13. Hansen, M.; Piprek, J.; Pattison, P.M.; Speck, J.S.; Nakamura, S.; DenBaars, S.P. Higher efficiency InGaN laser diodes with an improved quantum well capping configuration. *Appl. Phys. Lett.* **2002**, *81*, 4275–4277. [[CrossRef](#)]
14. Tansu, N.; Mawst, L.J. Current injection efficiency of InGaAsN quantum-well lasers. *J. Appl. Phys.* **2005**, *97*, 054502. [[CrossRef](#)]
15. Margetis, J.; Zhou, Y.; Dou, W.; Grant, P.C.; Alharthi, B.; Du, W.; Wadsworth, A.; Guo, Q.; Tran, H.; Ojo, S.; et al. All group-IV Si-GeSn/GeSn/SiGeSn QW laser on Si operating up to 90 K. *Appl. Phys. Lett.* **2018**, *113*, 221104. [[CrossRef](#)]
16. Pan, J.L.; Fonstad, C.G. Theory, fabrication and characterization of quantum well infrared photodetectors. *Mater. Sci. Eng. R Rep.* **2000**, *28*, 65–147. [[CrossRef](#)]
17. Zhou, X.; Li, N.; Lu, W. Progress in quantum well and quantum cascade infrared photodetectors in SITP. *Chin. Phys. B* **2019**, *28*. [[CrossRef](#)]

18. Wu, W.; Bonakdar, A.; Mohseni, H. Plasmonic enhanced quantum well infrared photodetector with high detectivity. *Appl. Phys. Lett.* **2010**, *96*, 161107. [[CrossRef](#)]
19. Seeger, K. *Semiconductor Physics*; Springer Science & Business Media: Berlin/Heidelberg, Germany, 2013.
20. Sun, Q.; Wang, L.; Wang, Y.; Ma, Z.; Chen, H. Direct Observation of Carrier Transportation Process in InGaAs/GaAs Multiple Quantum Wells Used for Solar Cells and Photodetectors. *Chin. Phys. Lett.* **2016**, *33*, 103–106. [[CrossRef](#)]
21. Wu, H.; Ma, Z.; Jiang, Y.; Wang, L.; Yang, H.; Li, Y.; Zuo, P.; Jia, H.; Wang, W.; Zhou, J.; et al. Direct observation of the carrier transport process in InGaN quantum wells with a pn-junction. *Chin. Phys. B* **2016**, *25*, 117803. [[CrossRef](#)]
22. Li, Y.; Jiang, Y.; Die, J.; Wang, C.; Yan, S.; Wu, H.; Ma, Z.; Wang, L.; Jia, H.; Wang, W.; et al. Visualizing light-to-electricity conversion process in InGaN/GaN multi-quantum wells with a p–n junction. *Chin. Phys. B* **2018**, *27*, 097104. [[CrossRef](#)]
23. Yang, H.; Ma, Z.; Jiang, Y.; Wu, H.; Zuo, P.; Zhao, B.; Jia, H.; Chen, H. The enhanced photo absorption and carrier transport of InGaN/GaN Quantum Wells for photodiode detector applications. *Sci. Rep.-UK* **2017**, *7*, 43357. [[CrossRef](#)]
24. Lim, S.; Ko, Y.; Cho, Y. A quantitative method for determination of carrier escape efficiency in GaN-based light-emitting diodes: A comparison of open- and short-circuit photoluminescence. *Appl. Phys. Lett.* **2014**, *104*, 91104. [[CrossRef](#)]
25. Watanabe, N.; Mitsuhara, M.; Yokoyama, H.; Liang, J.; Shigekawa, N. Influence of InGaN/GaN multiple quantum well structure on photovoltaic characteristics of solar cell. *Jpn. J. Appl. Phys.* **2014**, *53*, 112301. [[CrossRef](#)]
26. Lang, J.R.; Young, N.G.; Farrell, R.M.; Wu, Y.-R.; Speck, J.S. Carrier escape mechanism dependence on barrier thickness and temperature in InGaN quantum well solar cells. *Appl. Phys. Lett.* **2012**, *101*, 181105. [[CrossRef](#)]
27. Schubert, M.F.; Xu, J.; Dai, Q.; Mont, F.W.; Kim, J.K.; Schubert, E.F. On resonant optical excitation and carrier escape in GaInN/GaN quantum wells. *Appl. Phys. Lett.* **2009**, *94*, 081114. [[CrossRef](#)]
28. Song, J.-H.; Kim, H.-J.; Ahn, B.-J.; Dong, Y.; Hong, S.; Song, J.-H.; Moon, Y.; Yuh, H.-K.; Choi, S.-C.; Shee, S. Role of photovoltaic effects on characterizing emission properties of InGaN/GaN light emitting diodes. *Appl. Phys. Lett.* **2009**, *95*, 263503. [[CrossRef](#)]
29. Wang, W.; Wang, L.; Jiang, Y.; Ma, Z.; Sun, L.; Liu, J.; Sun, Q.; Zhao, B.; Wang, W.; Liu, W.; et al. Carrier transport in III–V quantum-dot structures for solar cells or photodetectors. *Chin. Phys. B* **2016**, *25*, 097307. [[CrossRef](#)]
30. Zou, Y.; Honsberg, C.B.; Freundlich, A.; Goodnick, S.M. Simulation of Electron Escape from GaNAs/GaAs Quantum Well Solar Cells. In Proceedings of the 2014 IEEE 40th Photovoltaic Specialist Conference (PVSC), Denver, CO, USA, 8–13 June 2014.
31. Tang, X.; Li, X.; Yue, C.; Wang, L.; Deng, Z.; Jia, H.; Wang, W.; Ji, A.; Jiang, Y.; Chen, H. Research on photo-generated carriers escape in PIN and NIN structures with quantum wells. *Appl. Phys. Express* **2020**, *13*, 071009. [[CrossRef](#)]
32. Busch, P.; Heinonen, T.; Lahti, P. Heisenberg's uncertainty principle. *Phys. Rep.* **2007**, *452*, 155–176. [[CrossRef](#)]

Disclaimer/Publisher's Note: The statements, opinions and data contained in all publications are solely those of the individual author(s) and contributor(s) and not of MDPI and/or the editor(s). MDPI and/or the editor(s) disclaim responsibility for any injury to people or property resulting from any ideas, methods, instructions or products referred to in the content.